HKIE THE HONG KONG INSTITUTION OF ENGINEERS 香港工程師學會

The role of shading and window-to-wall ratio on the energy-saving potential and daylighting associated with thermochromic smart windows

Yin Hoi Chan[1], Thilhara Tennakoon[1, 2], Yi Zhang[2], Sau Chung Fu[3], Ka Chung Chan[1], Chili Wu[1] and Christopher Yu Hang Chao[1,4]
[1] Department of Building Environment and Energy Engineering, The Hong Kong Polytechnic University, Hong Kong, China
[2] Department of Mechanical Engineering, The University of Hong Kong, Pokfulam, Hong Kong
[3] Division of Science, Engineering and Health Studies, College of Professional and Continuing Education, The Hong Kong Polytechnic University, Hong Kong, China
[4] Department of Mechanical Engineering, The Hong Kong Polytechnic University, Hong Kong, China

ABSTRACT

Thermochromic smart windows (TSWs), which regulate their properties by switching reversibly between clear and tinted states based on the temperature variation, can passively alleviate energy wastage caused by energy-inefficient fenestration. This study on the energy-saving potential of TSWs not only provides new insights into the practical application but also their integration into modern building designs. Unlike previous studies that compare TSW performance using their optical indices, this work comprehensively evaluated the energy-saving and daylight performance of three advanced TSW materials-hydrogel, perovskite, and vanadium dioxide—using self-created EnergyPlus simulation models. The impacts of orientation, window-to-wall ratio (WWR), and roller shade (RS) on TSW performance were assessed under Hong Kong's cooling-dominated climate. The perovskite-TSW demonstrated superior energy-saving potential, achieving power savings of 11-35% while ensuring maximum working hours (75-89%) with desirable daylighting ($UDI_{500\text{-}2000}$). The study identified a range of WWR between 0.34 and 0.67 where balanced illumination between the centre and rear of the office were achieved with different windows across orientations. The findings suggest that high-performance glazing like TSWs can potentially negate the need for RS, and demonstrate the feasibility of adopting a multi-TSW configuration for different orientations, offering more efficient and optimistic solutions for building energy management.

KEYWORDS Building energy simulation; Thermochromic smart window; Perovskite; Hydrogel; Vanadium dioxide
CONTACT Ka Chung Chan oscar-kc.chan@polyu.edu.hk
Received 28 November 2024

1. Introduction

Building envelopes are fundamental components that serve as a barrier between interior and outdoor environments, protecting occupants from external hazards. Heat transfer through the envelope substantially impacts the energy required for indoor thermal comfort, and hence, inefficient façade design can lead to energy wastage of the HVAC system. Owing to urbanisation and the increasing occurrence of extreme weather, HVAC systems have been the most significant end uses in buildings in metropolitan and emerging cities. Buildings and construction sectors accounted for about one-third of global energy consumption in 2021, and the annual carbon emissions from buildings increased to approximately 10 *Gt* CO_2 (United Nations Environment Programme [UNEP], 2022). Therefore, it is not just essential but urgent to resolve energy inefficiency in buildings to combat the global energy crisis.

Abundant energy-saving strategies for building envelopes have been introduced to address the issues of HVAC systems. Fenestration—a major source of heat exchange in buildings (Xue et al., 2019)—can be managed with state-of-the-art glazing materials. For instance, thermochromic smart windows (TSWs), which can passively regulate their properties by dynamically alternating between clear (cold) and tinted (hot) states in response to temperature changes without additional energy input (Somani and Radhakrishnan, 2003, Tällberg et al., 2019), have emerged as a type of energy-saving fenestration (Chan et al., 2022). The performance of the thermochromic glazing materials (TC material) is characterised by their critical transition temperature (T_c), visible transmittance (T_{vis}, for wavelengths ranging from 0.33 to 0.78 μm) and solar transmittance (T_{sol}, for wavelengths ranging from 0.30 to 2.50 μm) in both clear and tinted states. Since solar radiation constitutes approximately 46% near-infrared radiation (NIR) in the 0.78-2.5 μm waveband as described by Vignola et al. (2019), which is predominantly responsible for interior heating, a large contrast in hot and cold NIR transmittances is highly desirable for TSWs. Conventional TSWs are generally vanadium dioxide (VO2)-based, whilst emerging thermo-responsive materials, including perovskites, hydrogels, liquid crystals (LCs), and ionic liquids (ILs), have been extensively investigated (Chan et al., 2022). The thermochromic effect of VO_2 occurs in the NIR region, while hydrogels exhibit excellent control in both the visible and infrared regions. As IL and LC can only regulate visible light (47% of insolation), VO_2, hydrogels, and perovskites will be the focus of this paper due to their desirable features. An ideal TSW possesses low transition temperature (T_c), and high visible transmittance (T_{vis}), and high solar modulation (ΔT_{sol}). Many studies have investigated these optical properties, and yet achieving one property usually comes at the expense of the other(s). To provide a broader picture in current development of advanced glazing, this paper expands the comparison of the performance of TSWs from different material groups. This study aims to provide more insight into their practicality and to implement objective comparisons in terms of energy and daylighting performance of three favourable TSW materials.

In this work, the energy performance of an office room with three different types of TSWs is simulated using EnergyPlus, which is whole-building energy simulation software (Crawley et al., 2001). Although prototype models of various building types are supplied with EnergyPlus, they do not accurately represent real-life buildings in (sub)tropical climates where cooling demand dominates, as they adopt the envelope and their material properties that are used in the United States. Additionally, standard EnergyPlus prototype models do not consider window shading devices, which can significantly impact the thermal load of buildings. Given that window shading devices and window-to-wall ratio (WWR) affect the indoor thermal load and daylight illuminance, and their influence on TSW performance varies depending on the spectral properties of windows, building types, and architectural aesthetics. this study employs self-created office models which utilise common building materials that are used in Hong Kong to:

- quantify the energy-saving potential of three types of TSWs in an office room at different orientations under a cooling-dominated climate using EnergyPlus,
- explore the compatibility of a TSW and window shading device,
- examine the role of WWR on power-saving performance,
- assess the daylight illuminance of different glazing systems,
- discuss the merits and limitations of three individual glazing materials (VO_2, hydrogel, and perovskite-based TSWs from the literature with a Tc of about 30°*C*), and
- investigate if a particular TSW is better suited to a humid subtropical climate.

2. Methodology

2.1. Selection of Thermochromic Smart Windows

Three TC materials (hydrogel, perovskite, and VO_2) are chosen as they have demonstrated promising energy-saving potential in many studies (Chan et al., 2022, Zhang et al., 2022). Hydrogel-based TSWs consist of cross-linked polymeric networks that are saturated with water, sandwiched between transparent substrates. Among the various hydrogel TC materials, poly(N-isopropylacrylamide) (PNIPAm) is by far the most promising due to its high modulation contrast and narrow hysteresis. The PNIPAm TSW (T_c at 30-31°*C*) proposed by Lin et al. (2022) is selected for this study. It exhibits an ultra-broadband thermochromism: a silver nanowire mesh embedded in the polymer allows for thermal modulation; it is, therefore, expected to provide superior savings. A triple-coated glazing material (T_c: 25-50°*C*) of hydrated $MAPbI_{3-x}Cl_x$ perovskite, cesium-doped tungsten trioxide (CWO, which harvests NIR-wavelength photons), and a low-emissivity (low-E-) layer is chosen (Liu et al., 2022). The CWO layer is NIR-activated for triggering the thermochromism of hydrated $MAPbI_{3-x}Cl_x$ perovskite at room temperature owing to its high NIR absorptance (~90%). It could, therefore, regulate heat gain from visible light and NIR under ambient conditions, while demonstrating mid-infrared emission of up to 0.3 that limits the radiative heat transfer between the TSW and the indoor environment. Besides, this work considers a tungsten-doped (1.16%) VO_2 layer sandwiched by ZrO_2 layers on glass substrates that transitions at 22°*C* (Bárta et al., 2020). This coating, prepared via scalable sputter deposition, demonstrated comparable optical properties to other VO_2 glazings that use more complicated fabrication methods (Zhou et al., 2012, Ye et al., 2013, Sun et al., 2013), along with a low T_c. The optical indices of these three TC materials are calculated using the transmission and reflectance spectra reported in the respective literature, and presented in Figure 1 and Table 1. Although the selected TSWs undergo a phase transition at slightly different temperatures, their T_c is close to the average temperatures of Hong Kong, indicating their feasibility in tropical climates.

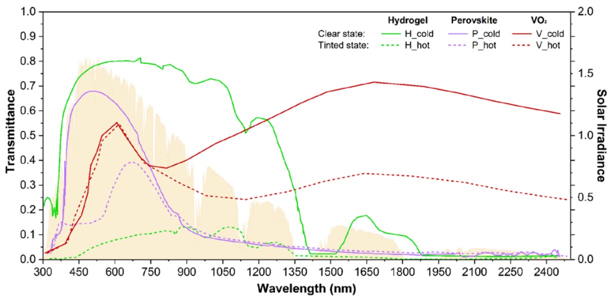

Figure 1. Transmittance spectra of the chosen hydrogel, perovskite, and VO_2 layers in cold (clear) and hot (tinted) states.

The TC-glass panel will incorporate an air gap and a low-E inboard glass into a double-glazed unit (DGU), and shorthand is used for each window system (Figure 2). Roller shade (RS) is one of the most frequently used internal window shading devices for glare control (Tzempelikos and Shen, 2013, Chan et al., 2015). Another three sets of TSW systems with an RS (denoted with "+RS") are used to

Table 1. Optical indices (fraction) of each glazing layer and roller shade for different window systems.

	Low-E	Clear	Hydrogel		Perovskite		VO_2		RS
			H_cold	H_hot	P_cold	P_hot	V_cold	V_hot	
Thickness (m)	0.002	0.003	0.006	0.006	0.004	0.004	0.001	0.001	0.005
Solar Transmittance	0.710	0.834	0.657	0.069	0.350	0.180	0.421	0.323	0.7
Solar Front Reflectance	0.190	0.075	0.076	0.554	0.090	0.090	0.157	0.178	0.
Solar Back Reflectance	0.190	0.075	0.076	0.554	0.110	0.110	0.157	0.178	0.2
Visible Transmittance	0.876	0.899	0.784	0.067	0.650	0.230	0.469	0.470	0.7
Visible Reflectance	0.092	0.083	0.070	0.750	0.110	0.100	0.067	0.117	0.2
IR Emissivity (Front)	0.840	0.840	0.920	0.920	0.780	0.780	0.840	0.840	0.9
IR Emissivity (Back)	0.068	0.840	0.350	0.920	0.270	0.300	0.840	0.840	0.9
Conductivity (W/mK)	1.000	1.000	0.240	0.240	0.900	0.900	0.900	0.900	0.1
Shade to glass distance (m)	-	-	-	-	-	-	-	-	0.05

Note: Low-E indicates a double-glazed unit with low-emissivity and clear glass panels; Clear indicates a double-glazed unit with clear glass panels; X_cold and X_hot represent the clear and tinted states of thermochromic glazing material (H: hydrogel, P: perovskite, and V: vanadium dioxide), respectively; RS denotes roller shade.

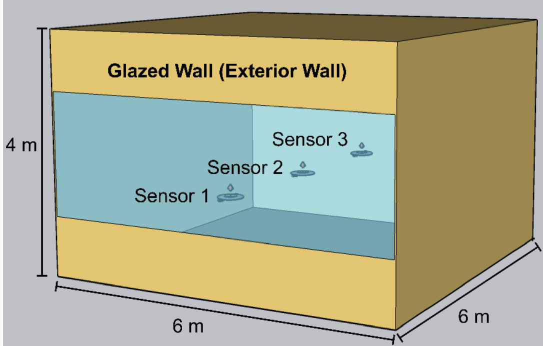

Configuration of Glazing and Building Envelope

Glazing System	Layer 1 (outboard)		Layer N [a] (inboard)	Internal Shade
Low-E_DGU+RS (Base case)	Clear glass	Air Gap (95% Argon, 5% Air)	Low-E glass	Roller Shade
HDGU	Hydrogen on PDMS tray and sealed with glass			-
HDGU+RS				Roller Shade
PDGU	Perovskite-CWO			-
PDGU+RS				Roller Shade
VDGU	$ZrO_2/V_{0.984}W_{0.016}O_2/ZrO_2$			
VDGU+RS				

[a] N denotes the serial number of layers for the respective glazing.

	Exterior Wall	**Interior Wall**	**Interior Ceiling/Floor**
Layer 1 (outermost)	Tile	Gypsum	Gypsum
	Cement/sand	Interior Concrete	C/F Concrete
	Exterior Concrete		
Layer N [a] (innermost)	Gypsum	Gypsum	C/F Tile
U-value [b]	2.135		-

[a] N denotes the serial number of layers for the respective facade; [b] The U-values of the exterior walls calculated by EnergyPlus.

Figure 2. Office model and façade configuration used in this work.

explore the influence of an RS on the performance of each TSW. A system consisting of DGU with clear and low-E glass panels and an RS, which can mimic typical window systems used in office buildings, serves as the reference case.

2.2. Simulation Model

An office room, which belongs to a commercial building, is created using SketchUp for conducting EnergyPlus simulation, where only the glazed façade is sun- and wind-exposed, while the others are treated as adiabatic, assuming that the spaces adjacent to the office model have similar thermal conditions (Figure 2). The U-value of the opaque exterior wall of the office complies with ASHRAE 90.1-2022 (ASHRAE, 2022) for Hong Kong (Climate Zone 1A). The model has a WWR of 0.5, which is the average WWR of office buildings in Hong Kong (Li and Tsang, 2008, Jia and Lee, 2018). In the later section of this study, a WWR of 0.2–0.7 is considered to investigate how the WWR affects the energy-saving feasibility of the TSWs.

Three daylighting sensors are installed to maintain daylight illuminance of 500 *lux*. For the glazing systems with an RS, the RS is assumed to be parallel to and cover all the glazing parts of the window when in place. Daylight illuminance was found to be a more suitable shading control strategy than incident solar radiation with respect to the lighting threshold and visual comfort (Tzempelikos and Shen, 2013). Hence, the RS is activated (on) if the total daylight glare index at sensor 1 (near the window) exceeds the maximum glare index specified in the daylighting input. The office is served by a centralised HVAC system with a cooling setpoint of 24°*C*. The year-round power consumption of the office is simulated using EnergyPlus, which uses a dedicated module for TC materials. The spectral characteristics in clear and tinted states are defined, and at each timestep of the simulation, the model considers the ambient conditions, internal heat loads, and heat transfer across the building envelope to calculate the TC layer's surface temperature, and thereafter assigns it the corresponding optical properties.

2.3. Assessment of Daylight Illuminance

Useful daylight illuminance (UDI) is one of the measures that indicates how often daylight illuminances within a range are achieved over a period of time (Nabil and Mardaljevic, 2006). This approach provides a straightforward yet comprehensive analysis of daylighting and solar penetration (Liang et al., 2018), and thus has been adopted in prior research (Tzempelikos and Shen, 2013, Liang et al., 2018). In this work, UDI is classified into three bins to evaluate the visual comfort with respective glazing systems between working hours (8:00-17:00) during weekdays (Monday to Friday):

(1) daylight illuminances between 0 and 500 *lux* ($UDI_{0\text{-}500}$) describe effectual but inadequate daylighting that is from a sole source of illuminance or depends heavily on artificial lighting,

(2) daylight illuminances in the range of 500-2000 *lux* ($UDI_{500\text{-}2000}$) provide occupants with desirable and satisfactory daylighting, and

(3) daylight illuminances of above 2000 *lux* ($UDI_{>2000}$) represent oversupplied daylighting that is likely to cause visual and/or thermal discomfort.

Moreover, balanced illuminance (BI), which indicates the specific WWR when the identical percentage of working hours with $UDI_{500\text{-}2000}$ at the centre (sensor 2) and rear-side (sensor 3) regions of the office is achieved, is identified.

3. Results and Discussion

3.1. Power-saving Performance of TSWs

The annual power consumption ranged from 2,384 to 3,573 *kWh* when the reference glazing unit (Low-E_DGU+RS) was adopted, with the east-facing and north-facing offices consuming the most and the least, respectively (Figure 3a). The three glazing systems, i.e., HDGU, PDGU, and VDGU, accomplished a total power saving of 8–29% across the four cardinal directions. PDGU outperformed the other TSWs in this study by mitigating energy consumption by 14–29%, excluding the west-facing office where HDGU had slightly higher savings (26% against 25%). Due to the hot and humid climate of Hong Kong, cooling was the dominant end use, accounting for 62–73% of total power consumption, while heating only contributed up to 0.2%. Since cooling was the governing end use, it was the main power-saving contributor (66–87% of total savings) and could thereby offset any penalty present (Figure 3b). For instance, even though the north-PDGU and north-VDGU obtained penalties through both heating (74–185%) and lighting (4–8%), they were compensated for by savings in cooling and fans, and positive overall savings were realised. As the TSWs have a lower T_{vis} in both clear and tinted states than the reference glazing, the offices that implement smart lighting—automatically dimming/brightening interior lights to meet the illuminance setpoint that is defined in the lighting schedule—risk lighting penalties when the TSWs are adopted. Additionally, increased lighting usage could precipitate an intensified cooling load due to the waste heat from lighting. While HDGU realised savings in cooling and fans, it induced the greatest increase in lighting power (20-30%) in all orientations compared to the other two TSWs, slightly reducing the overall savings.

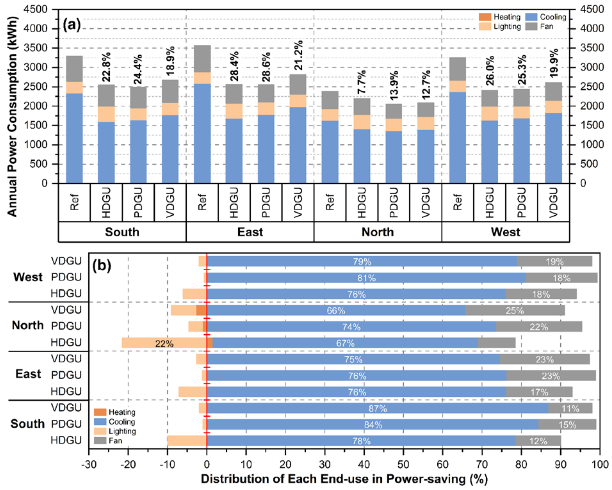

Figure 3. (a) Annual power consumption and percentage of power saved (labels) by different window systems; (b) Contribution of each end use in power saving.

The magnitude of power saving in HVAC systems significantly depends on the window's A_{sol} and $T_{sol,\text{hot}}$ which substantially impact the window's surface temperature as TSW switches state in response to temperature stimuli. The energy saving potential of TSW is a direct consequence of the TSW's switching behaviour, which is influenced by the window surface temperature, which in turn is a function of its spectral properties (most notably, A_{sol}), and solar radiation received by the window. In this study, the temperature of the thermochromic (TC) layer of respective TSWs varied between 9°*C* and 72°*C*. Regardless of TSW type, the maximum TC layer temperatures of the north-facing TSWs were around 40°*C*, which were much lower than when facing the other orientations where they achieved higher maximum temperatures of around 48–72°*C*. Consequently, the south and east TSWs switched to their tinted states more often as they received significantly more solar irradiation (annual average of 111 W/m^2). Among all three TSWs, the TC layer of PDGU reached the highest temperatures across all orientations. Due to its NIR-harvesting CWO coating, PDGU had the highest A_{sol} ($A_{sol,cold}$: 0.560, $A_{sol,hot}$: 0.730) and exhibited the fastest heating response (Figure 4). Windows with a sufficiently high A_{sol} can reach its T_c and even exist in the tinted state despite the ambient temperature being below the window's transition temperature as a result of incident solar radiation absorption, thereby leading to increased instances of switching/tinting during the cooling period. This is beneficial as the outdoor temperature of 25–30°*C* (below the T_c of some TSWs) already warrants indoor cooling. As is evident in Figure 5, HDGU and PDGU could switch to the tinted state when the solar irradiation was strong enough (>100 W/m^2) to trigger thermochromism, despite having a T_c that is higher than the outdoor dry-bulb temperature: especially PDGU whose T_c is 37.5°*C*. Nevertheless, PDGU despite its high A_{sol} spent less than 20% of the time in the tinted state given its high T_c. While this may be disadvantageous in cooling demand situations, it can help prevent excessive tinting when lighting and heat

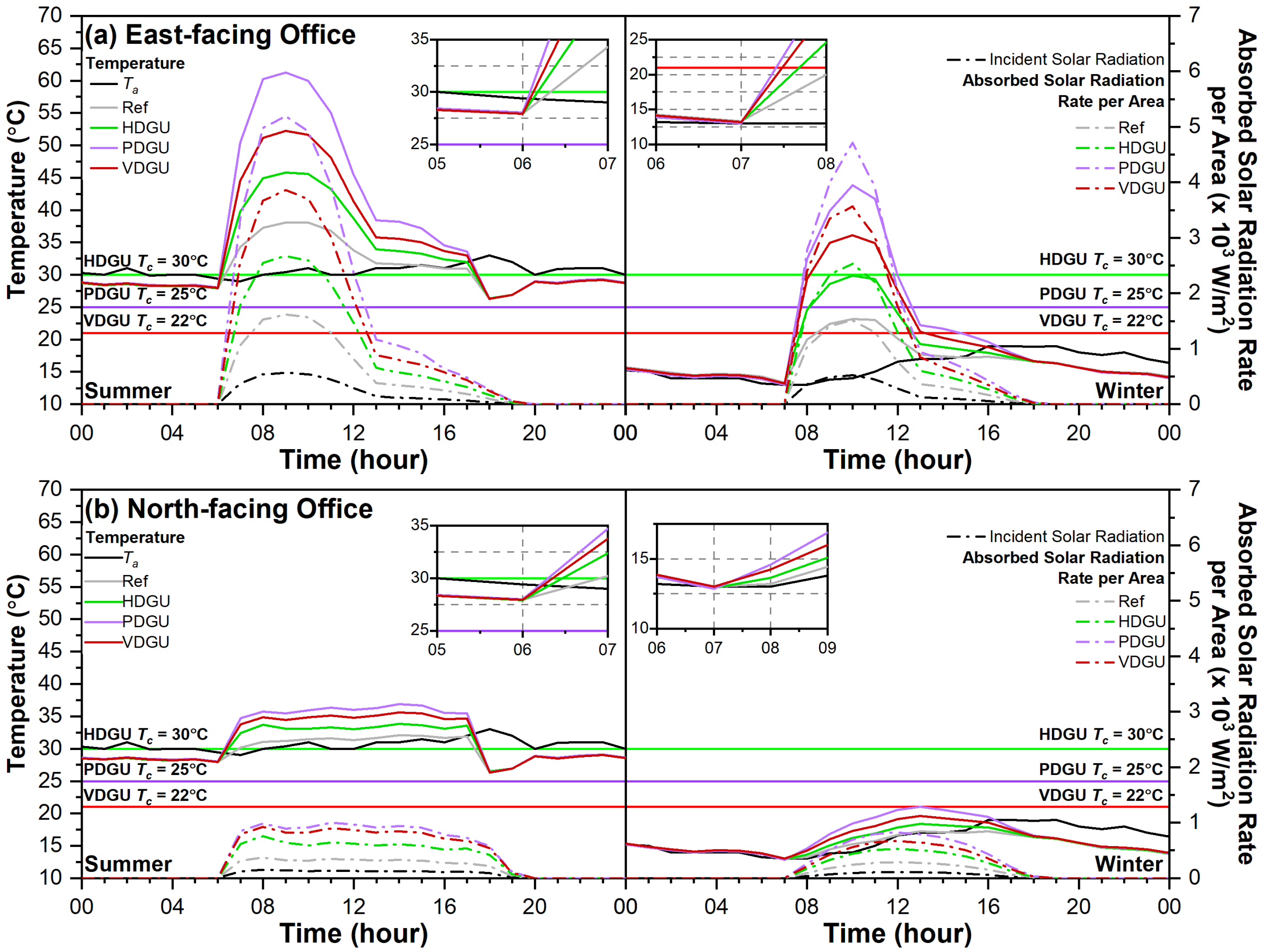

Figure 4. Window surface temperature and absorbed solar radiation rate per area at (a) east- and (b) north-facing offices on a typical day in summer and winter.

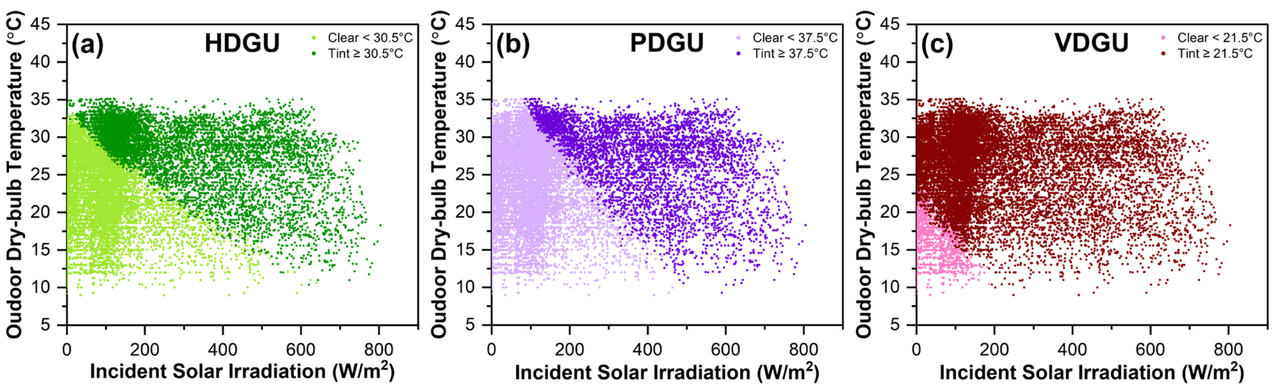

Figure 5. Incident solar irradiation and outdoor dry-bulb temperature that correlatedly lead to the clear or tinted state of (a) HDGU, (b) PDGU, and (c) VDGU for all orientations. Thermochromic state of the TSW is interpreted by scatter colour.

gain are needed during periods of low ambient temperature and inadequate solar irradiation (e.g., morning and sunset). Conversely, owing to its low T_c (22°C) and high A_{sol}, VDGU spent 72–78% of the time in the tinted state (Figure 5).

3.2. Influence of RS on Power Saving and Daylighting Performance of TSWs

The addition of an RS reduced the overall power saving by 3–69%, with the two exceptions of the north-HDGU+RS and north-PDGU+RS, where the saving was improved. The results showed that an RS diminished the savings in heating or magnified the heating penalty, e.g., the east-facing PDGU could achieve 71% savings in heating, while PDGU+RS resulted in a penalty of 46%. Additionally, the lighting penalty was amplified by 0.1–1% for HDGU(+RS), while it remained effectively unchanged for VDGU(+RS) and PDGU(+RS). Regardless of the presence of an RS, the power saved by TSWs significantly hinges on the window heat gain driven by spectral properties and factors such as orientation and solar irradiation. For Hong Kong, located in the northern hemisphere, the incident solar radiations of the south-, east- and west-facing windows were discovered to be more pronounced, which is in accordance with Rosado and Levinson (2019). Window heat gain is the sum of transmitted incident solar energy (direct heat gain), and the energy is absorbed by glazing and transferred to the building space via conduction, convection, and radiation (indirect heat gain). The office facing various orientations undergo different scales of solar irradiation over a year. The south-facing office receives the most substantial heat gain during winter, while the north-facing office experiences the peak during summer (Table 2). When TSWs come into play, TC materials with a high $T_{sol,cold}$ and $A_{sol,cold}$ play crucial corresponding roles in direct and indirect passive heating. All three TC materials have a lower $T_{sol,cold}$ than the clear glass of the baseline Low-E_DGU (0.834), thereby alleviating the direct heat gain and total window heat gain by 32–57% on average (Table 2), which is consistent with the total power savings by various TSWs. Although TSW+RS mitigated the heat gain with respect to the Low-E_DGU+RS, the RS increased the window's heat gain compared to cases with TSW alone in most scenarios (Table 2). Among the three TSWs, the HDGUs typically demonstrated a larger increase of about 22–44% in heat gain after implementing RS. However, the north-H/PDGU+RS showed a slightly lower average heat gain of 3–12.5% than in the H/PDGU cases.

The RS of the Low-E_DGU+RS operated for 93–98% of the working hours across different orientations, during which it was turned on the most in the south-facing office. Given that the chosen TSWs have a relatively lower T_{vis} in both states, replacing the Low-E_DGU with the TSWs significantly decreased the number of occupied hours with the RS being active. The non-operating time of the RS was increased to 34% and 40% for HDGUs in the south- and north-facing offices against the base cases (2% and 6%), respectively, which can be attributed to its low $T_{vis,hot}$ (0.067). The non-operating hours of the RS was increased remarkably during the cooling period (April to October). In contrast, it was less influenced by the TSWs during winter, excluding the north-facing VDGU (Table 3). This could be due to the VDGU having the lowest T_c, such that it remains tinted for a longer period of time than the other two TSWs when ambient temperatures are lower in winter. Thus, it was preferred for the RS to be inactive for desired daylighting when the TSWs were tinted. The results mentioned above reveal that the RS and shading control strategy utilised in this study compromised power saving with magnified window heat gain. Hence, RS might not be necessary when TSWs are adopted in the first place, which is in agreement with Tzempelikos and Shen (2013). They concluded that when advanced glazing with low transmittance is used, open/closed shading becomes inefficient and thus is not recommended.

Table 2. Annual window heat gain of each glazing at the south- and north-facing offices.

South	HDGU	PDGU	VDGU
	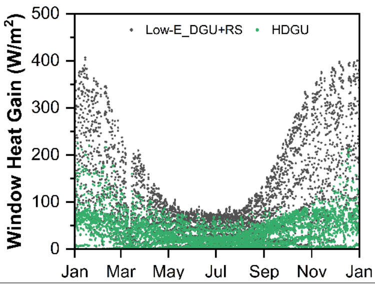	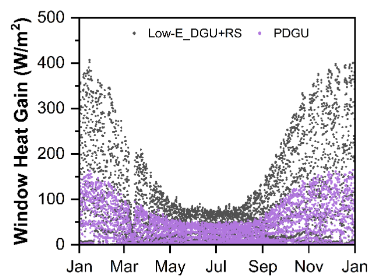	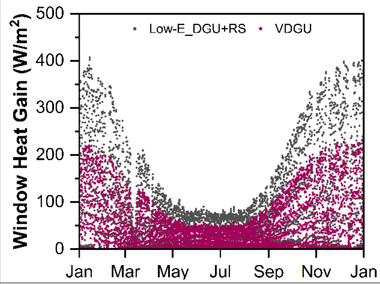
	HDGU+RS	PDGU+RS	VDGU+RS
	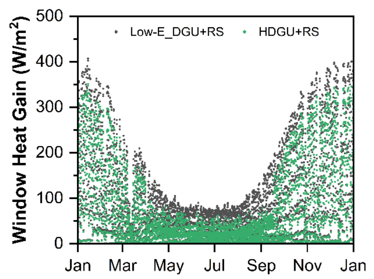	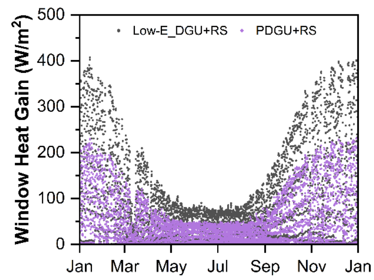	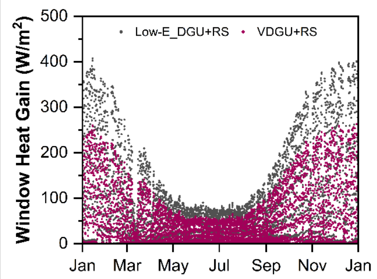
North	HDGU	PDGU	VDGU
	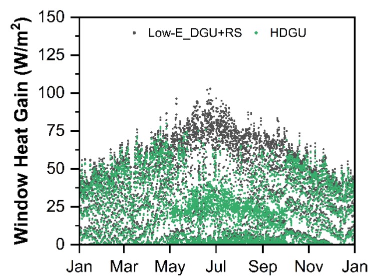	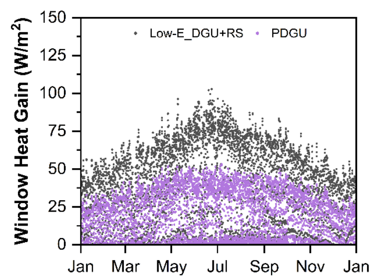	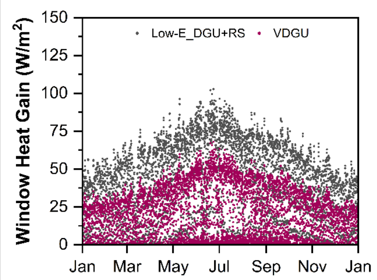
	HDGU+RS	PDGU+RS	VDGU+RS
	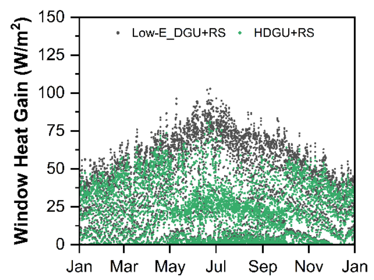	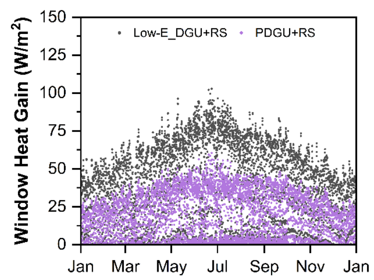	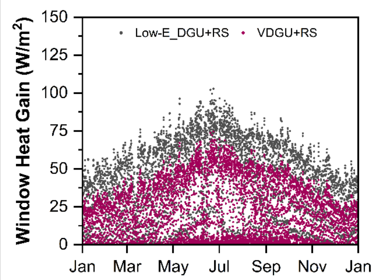

Table 3. Temporal plot of the roller shade opening fraction during working hours (Monday to Friday, 8:00–17:00) with different window systems.

	South [a]	North [a]
Low-E_DGU+RS	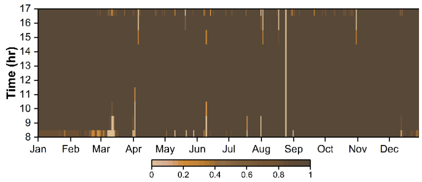	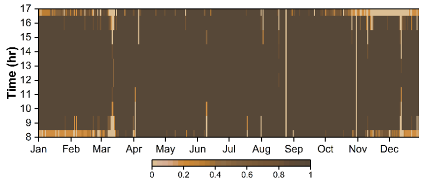
HDGU+RS	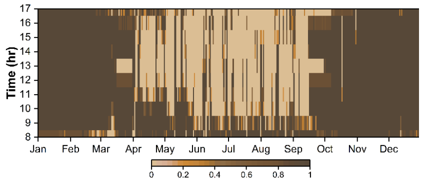	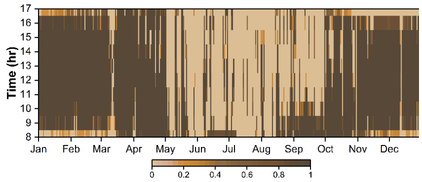
PDGU+RS	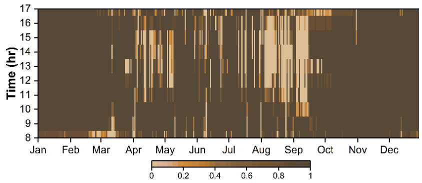	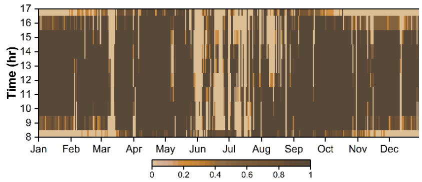
VDGU+RS	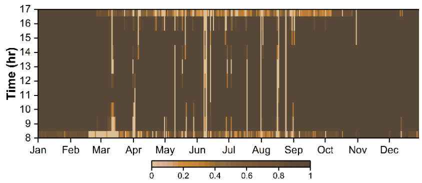	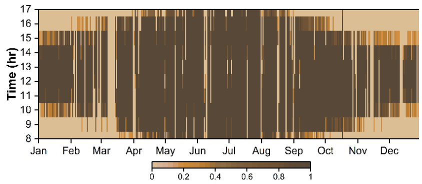

[a] The colour ramp indicates the opening fraction in an hour from 0.0 (unswitched, beige) to 1.0 (fully switched, brown).

In the reference cases, occupants would predominantly experience oversupplied daylighting ($UDI_{>2000}$) for more than 90% of office hours at sensor 1, despite which orientation the window faced. When TSW(+RS) systems were utilised, the percentage of undersupplied daylighting ($UDI_{0\text{-}500}$) during occupied hours was unsurprisingly increased at all sensors owing to their lower T_{sol} and T_{vis} against the Low-E_DGU regardless of orientation. This caused less daylight to penetrate through the glazing, which, in turn, caused a reduction in hours of $UDI_{>2000}$ and an increase or decrease in useful daylighting ($UDI_{500\text{-}2000}$) depending on the monitored regions. Different TSW systems accomplished optimal percentages of $UDI_{500\text{-}2000}$ at varying distances from the window for different offices (Figure 6). At sensor 1, the percentage of $UDI_{500\text{-}2000}$ was enhanced the most to ~25% by HDGU(+RS) in the south-facing office, while it was accomplished by VDGU(+RS) to 36.7–55.1% in the other offices. This could be due to VDGU spending more hours in the tinted state when its $T_{vis,hot}$ (0.470) is lower than $T_{vis,cold}$ of the other two TSWs (H_cold: 0.784 and P_cold: 0.650). In contrast, $UDI_{500\text{-}2000}$ was improved at the centre and rear side of the room, excluding the north-facing office, where the percentage reduced with all TSW(+RS) (Figure 6). In addition, the working hours of $UDI_{0\text{-}500}$ at regions distant from the window were increased dramatically with TSW(+RS), especially in the north-facing offices. Nonetheless, the adoption of TSW substantially diminished the hours of $UDI_{>2000}$, and they reduced the percentage of $UDI_{>2000}$ at sensors 2 and 3 in the north-facing offices (Figure 6). Further, the percentages of working hours of different UDI bins between TSW and TSW+RS scenarios were fairly identical, especially between VDGU and VDGU+RS or when H/PDGU(+RS) were applied in north-facing offices that received the least sunlight (Figure 6). Besides, the deployment of an RS in the TSW systems did not improve and could reduce the number of office hours of $UDI_{500\text{-}2000}$ in some cases.

As the addition of RS to TSW systems reduced power saving and negligible variation in UDI level, the section (Section 3.3) hereinafter will address the glazing units with only TSW at different WWRs.

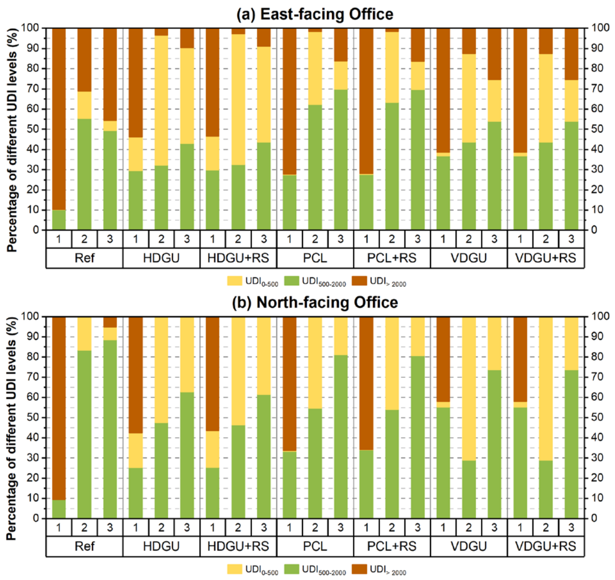

Figure 6. Percentage of different UDI levels at sensors 1, 2, and 3 in the (a) east- and (b) north-facing offices with various window systems.

3.3. Effect of Window-to-wall Ratio on TSW Performance

All window systems reported mitigation in total power intensity with respect to the reference case with increasing WWR in different orientations, albeit that the north-HDGU_0.2 (X in "_X" represents a specific WWR) enhanced the total power intensity by 0.7% (Table 4). In the south- and north-facing offices that received the most and least solar irradiation, PDGU surpassed the other TSWs by achieving maximum power saving of 3–33%, and demonstrated more pronounced savings when facing south. In the east- and west-facing offices, PDGU was outperformed by HDGU when the WWRs were 0.6–0.7 (east) and 0.5–0.7 (west). HDGU was the only TSW that did not incur heating penalty among the three TSWs in all orientations. The other two TSWs intensified the heating demand, although this was easily offset by savings for other end uses, as heating is not the governing end use. More importantly, the TSWs could exponentially reduce the cooling power intensity with increasing WWR. Although HDGU (5–42%) and PDGU (7–37%) demonstrated competitive power saving performance in cooling, the former showed slightly higher savings in different orientations except for the north-facing office (Table 4). Regardless of glazing type, the lighting penalty was alleviated by increasing the WWR. When identical TSWs were utilised, the least lighting penalty was achieved in the west-facing office for all PDGUs and HDGU_0.4/0.5/0.6/0.7. In particular, the south-facing HDGU spent 15–49% more working hours in its opaque state ($T_{vis,hot}$: 0.067) than in the remaining offices, which led to a stronger reliance on artificial lighting and as such, was associated with the highest penalties.

As it is harder for incident sunlight to reach the centre or rear side of the room (sensor 2 or 3), occupants located further away from the window would require artificial daylighting to satisfy their visual demand. Any effort to increase $UDI_{500\text{-}2000}$ working hours at one location was found to cause a variation in the other (Table 4). For the Low-E_DGU+RS with the highest T_{sol} and T_{vis} among all windows, increasing the WWR increased the oversupplied hours, and consequently reduced working hours with adequate daylighting as unrestricted sunlight is admitted into the offices. The optimum percentages of $UDI_{500\text{-}2000}$ (55–90% with a WWR of 0.3–0.6) were achieved at sensors 2 and 3. When TSWs were deployed, the regions at sensors 2 and 3 were mostly undersupplied by daylight since the TSWs had lower T_{vis} in both cold and hot states than the Low-E_DGU. This is more evident in the north-facing offices, which receive the least sunlight. Although more daylight penetration was allowed when increasing WWR, any growth in oversupplied daylighting could easily be outweighed by the improvement in undersupplied and adequate daylighting at sensors 2 and 3. The studied TSWs appeared to ameliorate the daylighting distribution within the office with increasing WWR, which did not occur in the reference cases. Unlike conventional glazing, incident sunlight is not the only factor that affects the daylighting illuminance in the TSW cases due to their temperature-stimulated phase switching characteristic. Thus, the WWR that accomplished peak $UDI_{500\text{-}2000}$ varied distinctively at different orientations depending on the glazing (Table 4). The percentage of $UDI_{500\text{-}2000}$ at sensor 2 improved with WWR across orientations, whilst it could reach the optimum with a specific WWR at sensor 3. Daylighting in one of these two regions would be satisfied at the expense of the other region where undersupplied or oversupplied daylighting working hours would be affected. This could be attributable to the fact that the solar radiation received at the rear of the office was significantly limited and/or the glazing utilised had a relatively low T_{vis}, such that artificial lighting would be needed when natural daylight is insufficient. For instance, oversupplied working hours at sensor 3 with P/VDGU_0.4 near doubled to the WWR of 0.5 that achieved optimal $UDI_{500\text{-}2000}$ from the previous WWR (0.4).

Table 4. Annual power intensity and percentage of UDI500–2000 with different glazing systems at a WWR of 0.2–0.7 in the south- and north-facing offices.

<table>
<tr><td></td><td>South [a]</td><td>North [a]</td></tr>
<tr><td>Low-E_DGU+RS</td><td>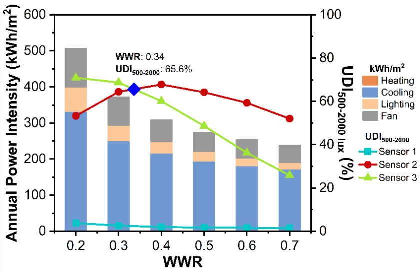
</td><td>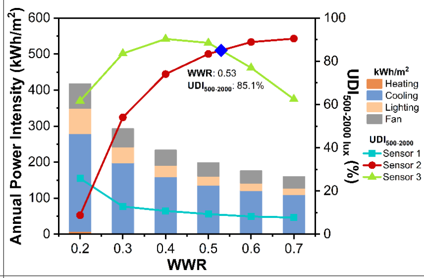
</td></tr>
<tr><td>HDGU</td><td>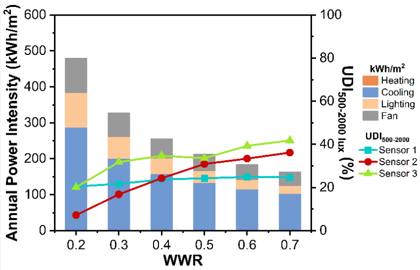
</td><td>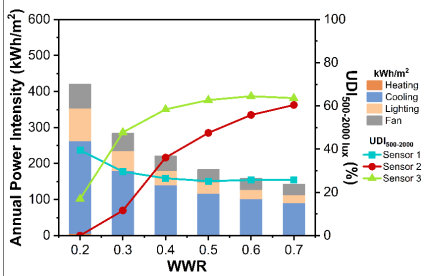
</td></tr>
<tr><td>PDGU</td><td>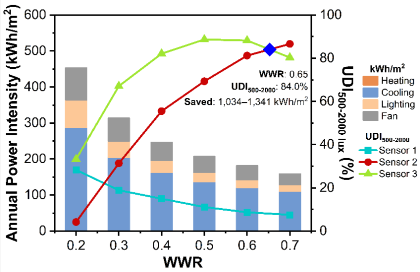
</td><td>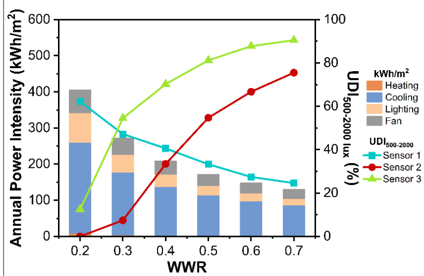
</td></tr>
<tr><td>VDGU</td><td>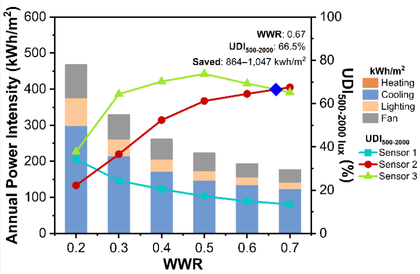
</td><td>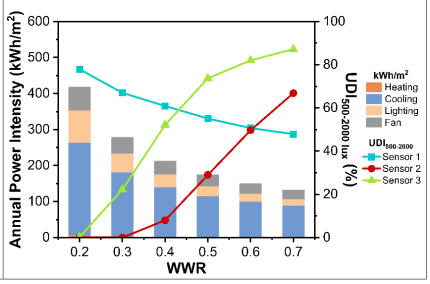
</td></tr>
</table>

[a] Blue diamond with labels indicates the balance illuminance between sensors 2 and 3 with an estimated range of power saving

To identify the WWR at which the office is evenly illuminated, the parameter, balanced illuminance (BI), is adopted. When the ratio of adequate daylighting ($UDI_{500-2000}$) hours between sensors 2 and 3 is one (the intersection of the curves in the graphs in Table 4). BI is achieved. The reference glazing attained identical $UDI_{500-2000}$ of 66% and 85% at both sensors 2 and 3 with WWRs of 0.34 (south) and 0.53 (north) (Table 4).For the south-PDGU and south-VDGU, BI occurred at similar WWRs (0.65 against 0.67), albeit that the former achieved a much higher $UDI_{500-2000}$ of 84.0% and power saving of 1,034–1,341 kWh/m^2 than the latter (66.5% and 864–1,047 kWh/m^2). PDGU could guarantee its power-saving performance with a high level of satisfactory daylighting at multiple regions of a room. HDGU was found to require a higher WWR (above 0.7) to achieve BI, which is unrealistic for typical office buildings. Moreover, given that the north-facing offices receive only half of the solar irradiation of the other offices, the percentages of $UDI_{500-2000}$ remained increasing with WWR when the north-TSWs were adopted, and BI was not achieved at a WWR below 0.7. The above-mentioned results reveal that identical daylighting illuminance at different regions of a room is difficult to achieve or is often fulfilled at the cost of increasing undersupplied or oversupplied daylighting hours and the use of artificial light depending on the spectral properties of the glazing type and orientation, which may lead to glare discomfort in certain areas of the room and lighting penalty respectively.

4. Conclusion

This study explored the energy-saving potential of three thermochromic smart windows (TSWs) developed using respective TC materials—hydrogel, perovskite, and vanadium dioxide—under cooling-dominated weather. The impact of the window-to-wall ratio (WWR) on energy saving and daylighting performance of glazings was also examined. The three TSWs demonstrated significant power saving by reducing solar penetrance and window heat gain. PDGU, which could harvest NIR photons for phase transition, outperformed others in most cases, especially in the south- and north-facing offices that received the most and least sunlight, respectively, achieving an optimal power saving of 11–35% across various orientations. However, in the east- and west-facing offices, HDGU exhibited the greatest performance at WWRs ≥ 0.5 over PDGU, suggesting that the optimal configuration involves a multi-TSW approach tailored to different orientations. Although VDGU showed comparatively less prominent savings than the other two TSWs, its relatively low T_c (22°*C*) and high $T_{vis,hot}$ (0.470) allowed it to be tinted for at least twice the tinted hours of the other two TSWs, while retaining lighting penalty at a mediate level. The UDI approach was used to analyse how the visual comfort during working hours was affected in different scenarios. Since various parameters, including spectral properties of windows and orientation, contribute to daylighting illuminance, balanced illuminance (BI) between the centre (sensor 2) and rear-side (sensor 3) of the room with identical $UDI_{500\text{-}2000}$, was identified for an extensive range of WWRs for some of the glazing systems studied in this work. BI was achieved at WWRs between 0.34 and 0.67, depending on the window type and orientation. PDGU demonstrated its practicability in power saving, while ensuring sufficient desirable and balanced daylight illuminance between different regions of the room. Although larger window areas can permit the entry of natural light into the workplace, unrestricted solar radiation into buildings can lead to unbearable heat gain, escalating cooling demand and extreme glare. This necessitates the use of shading devices such as roller shades (RSs). The addition of RSs to TSW systems decreased the power saving and $UDI_{500\text{-}2000}$ hours with reduced RS operation hours, suggesting that advanced glazing may render such shading devices unnecessary. Many TSWs, such as those studied in this work, can preserve outdoor views while mitigating heat gain and building power consumption regardless of their thermochromic states, unlike RS, which do not provide the same level of visibility. With that being said, shading devices like roller shades can be controlled by occupants' willingness, while TSWs regulate their states based on temperature variation, and hence, the latter may not be freely managed upon occupants' desire.

This study highlighted the potential of hybrid TSWs that exploit broadband thermochromism for greater energy efficiency. Recent developments in the field have also shown smart windows that are integrated with air-cleaning and self-cleaning capabilities, as well as energy harvesting and storage. These state-of-the-art technologies can boost TSW's appeal and foster the collective goal of net-zero buildings. However, more research is needed on the cost and scalability of these smart glazing materials, along with their long-term stability, which has remained challenging. Future work shall also aim to access the energy-saving potential and cost-effectiveness (payback threshold) of TSWs in other building types such as residential and industrial buildings that have a wide variety of operating schedules, on the premise of fulfilling government guidelines and regulations.

Acknowledgements

This work was supported by the Research Impact Fund [grant number R1018-22], the Research Grants Council of the Hong Kong Special Administrative Region, China, the Policy Research Centre for Innovation and Technology (PReCIT), The Hong Kong Polytechnic University, Financial Support for Non-PAIR Research Centres [Projects no. PolyU P0043833], and Start-up Fund for RAPs under the Strategic Hiring Scheme from PolyU (UGC) [Projects no. PolyU P0046277]. This work was also funded by the Environment and Conservation Fund [Project No. 35/2022].

Notes on contributors

Ms Yin Hoi Chan is currently a Research Associate at the Department of Building Environment and Energy Engineering, The Hong Kong Polytechnic University. She received her MEng degree in Chemical Engineering at Swansea University, United Kingdom. Her research fields cover passive radiative cooling, energy-efficient building, and building energy simulation.

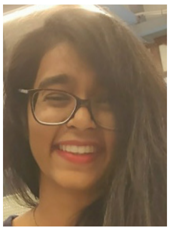

Ms Thilhara Tennakoon is now a Ph.D. candidate in the Department of Mechanical Engineering at The University of Hong Kong, and a Research Associate at the Department of Building Environment and Energy Engineering, The Hong Kong Polytechnic University. She received her BEng and MSc degrees from The University of Hong Kong in 2019 and 2023. Her research interests include passive cooling technologies, acoustophoresis, nano-energy, and aerosols.

Dr Yi Zhang is a Postdoctoral Research Fellow at the Department of Mechanical Engineering, The University of Hong Kong. He earned his Ph.D. degree from the University of Hong Kong in 2019. His research interests encompass thermal management, mechanical energy harvesting, and thermochromic smart windows.

Dr Sau Chung Fu is a Lecturer at the College of Professional and Continuing Education, The Hong Kong Polytechnic University. He received his BEng and MPhil in Mechanical Engineering from the University of Hong Kong, and pursued a Ph.D. degree in Mechanical Engineering at the Hong Kong Polytechnic University. He was a research associate at the Hong Kong University of Science and Technology, a postdoctoral fellow and a research assistant professor at the HKUST Fok Ying Tung Graduate School, and a research assistant professor in the Department of Mechanical Engineering, HKU. His research focuses on acoustics, thermofluids, aerosols, indoor air quality, and energy efficient building, using numerical simulations as well as advanced experimental techniques.

Dr Ka Chung Chan is a Research Assistant Professor at The Hong Kong Polytechnic University. He received his Bachelor, MPhil, and Ph.D. degrees in Mechanical Engineering from The Hong Kong University of Science and Technology. He was appointed as Research Assistant Professor in HKUST Fok Ying Tung Graduate School and engaged in postdoctoral research at the postdoctoral workstation of Nansha Information Technology Park, Guangzhou. His research area includes energy and thermal systems, adsorption technology, energy sustainability, and thermal fluidic simulation.

Dr Chili Wu is currently a Senior Research Fellow in the Department of Building Environment and Energy Engineering, Manager of the Policy Research Centre for Innovation and Technology at The Hong Kong Polytechnic University. He is also a member of the All-China Youth Federation in Hong Kong, and serves as the Executive Chairman of the Hong Kong Young Scientists Association. He has presided over or participated in science and technology funding projects from the national government, HKSAR, Guangdong Province, Guangzhou City, and business cooperation projects in Hong Kong, Mainland China, and South Korea. His main research areas cover new energy utilisation, improving energy efficiency, and energy-saving technology, improving the indoor air environment, and improving ventilation systems.

Prof Christopher Yu Hang Chao is the Senior Vice President (Research and Innovation), Chair Professor of Thermal and Environmental Engineering, Director of Policy Research Centre for Innovation and Technology (PReCIT) at The Hong Kong Polytechnic University. He obtained his M.S. and Ph.D. degrees in Mechanical Engineering from The University of California, Berkeley, USA. Prof. Chao joined the HKU to serve as Dean of Engineering and Chair Professor of Mechanical Engineering (2018–2021). He serves as Editor and is on the editorial boards of several major journals in the field of Energy and Built Environment including Energy and Buildings, Building and Environment, etc. Prof. Chao serves in various government units and core I&T organisations including the New Energy Transport Fund and Gas Safety Advisory Committee of the Hong Kong Environment Bureau, the Building Committee of the Housing Authority, etc. His major research fields include aerosol and gaseous contaminant transport in indoor environments, solar and waste heat-driven cooling and refrigeration systems, passive radiative cooling, nanofluid heat transfer, bio-inspired heat transfer, and fire dynamics and combustion.

References

[1] Ashrae 2022. *ANSI/ASHRAE/IES Standard 90.1-2022 Energy Standard for Sites and Buildings Except Low-Rise Residential Buildings (SI Edition)*. Peachtree Corners, Georgia: ASHRAE.

[2] Bárta, T., Vlček, J., Houška, J., Haviar, S., Čerstvý, R., Szelwicka, J., Fahland, M. & Fahlteich, J. 2020. Pulsed magnetron sputtering of strongly thermochromic VO_2-based coatings with a transition temperature of 22°C onto ultrathin flexible glass. *Coatings*, 10, 1258.

[3] Chan, Y.-C., Tzempelikos, A. & Konstantzos, I. 2015. A systematic method for selecting roller shade properties for glare protection. *Energy and Buildings*, 92, 81–94.

[4] Chan, Y. H., Zhang, Y., Tennakoon, T., Fu, S. C., Chan, K. C., Tso, C. Y., Yu, K. M., Wan, M. P., Huang, B. L. & Yao, S. 2022. Potential passive cooling

methods based on radiation controls in buildings. *Energy Conversion and Management*, 272, 116342.

[5] Crawley, D. B., Lawrie, L. K., Winkelmann, F. C., Buhl, W. F., Huang, Y. J., Pedersen, C. O., Strand, R. K., Liesen, R. J., Fisher, D. E. & Witte, M. J. 2001. EnergyPlus: creating a new-generation building energy simulation program. *Energy and Buildings*, 33, 319–331.

[6] Jia, J. & Lee, W. L. 2018. The rising energy efficiency of office buildings in Hong Kong. *Energy and Buildings*, 166, 296–304.

[7] Li, D. H. & Tsang, E. K. 2008. An analysis of daylighting performance for office buildings in Hong Kong. *Building and Environment*, 43, 1446–1458.

[8] Liang, R., Sun, Y., Aburas, M., Wilson, R. & Wu, Y. 2018. Evaluation of the thermal and optical performance of thermochromic windows for office buildings in China. *Energy and Buildings*, 176, 216–231.

[9] Lin, C., Hur, J., Chao, C. Y., Liu, G., Yao, S., Li, W. & Huang, B. 2022. All-weather thermochromic windows for synchronous solar and thermal radiation regulation. *Science Advances*, 8, eabn7359.

[10] Liu, S., Li, Y., Wang, Y., Yu, K. M., Huang, B. & Tso, C. Y. 2022. Near-infrared-activated thermochromic perovskite smart windows. *Advanced Science*, 9, 2106090.

[11] Nabil, A. & Mardaljevic, J. 2006. Useful daylight illuminances: A replacement for daylight factors. *Energy and Buildings*, 38, 905–913.

[12] Rosado, P. J. & Levinson, R. 2019. Potential benefits of cool walls on residential and commercial buildings across California and the United States: Conserving energy, saving money, and reducing emission of greenhouse gases and air pollutants. *Energy and Buildings*, 199, 588–607.

[13] Somani, P. R. & Radhakrishnan, S. 2003. Electrochromic materials and devices: present and future. *Materials Chemistry and Physics*, 77, 117–133.

[14] Sun, Y., Xiao, X., Xu, G., Dong, G., Chai, G., Zhang, H., Liu, P., Zhu, H. & Zhan, Y. 2013. Anisotropic vanadium dioxide sculptured thin films with superior thermochromic properties. *Scientific Reports*, 3, 1–10.

[15] Tällberg, R., Jelle, B. P., Loonen, R., Gao, T. & Hamdy, M. 2019. Comparison of the energy saving potential of adaptive and controllable smart windows: A state-of-the-art review and simulation studies of thermochromic, photochromic and electrochromic technologies. *Solar Energy Materials and Solar Cells*, 200, 109828.

[16] Tzempelikos, A. & Shen, H. 2013. Comparative control strategies for roller shades with respect to daylighting and energy performance. *Building and Environment*, 67, 179–192.

[17] United Nations Environment Programme (UNEP) 2022. *2022 Global Status Report for Buildings and Construction: Towards a Zeroemission, Efficient and Resilient Buildings and Construction Sector*. Nairobi.

[18] Vignola, F., Michalsky, J. & Stoffel, T. 2019. *Solar and Infrared Radiation Measurements*. CRC Press.

[19] Xue, P., Li, Q., Xie, J., Zhao, M. & Liu, J. 2019. Optimization of window-to-wall ratio with sunshades in China low latitude region considering daylighting and energy saving requirements. *Applied Energy*, 233, 62–70.

[20] Ye, H., Long, L., Zhang, H., Xu, B., Gao, Y., Kang, L. & Chen, Z. 2013. The demonstration and simulation of the application performance of the vanadium dioxide single glazing. *Solar Energy Materials and Solar Cells*, 117, 168–173.

[21] Zhang, Y., Tennakoon, T., Chan, Y. H., Chan, K. C., Fu, S. C., Tso, C. Y., Yu, K. M., Huang, B. L., Yao, S. H. & Qiu, H. H. 2022. Energy consumption modelling of a passive hybrid system for office buildings in different climates. *Energy*, 239, 121914.

[22] Zhou, S., Li, Y., Zhu, H., Sun, R., Zhang, Y., Huang, Y., Li, L., Shen, Y., Zhen, Q. & Tong, G. 2012. Microstructures and thermochromic characteristics of low-cost vanadium–tungsten co-sputtered thin films. *Surface and Coatings Technology*, 206, 2922–2926.